Passive shape shifting

A compliant design approach for full film bearings

Nijssen, Joep; van Ostayen, Ron

DOI
10.1177/09544062211003616

Publication date
2021

Document Version
Final published version

Published in
Proceedings of the Institution of Mechanical Engineers, Part C: Journal of Mechanical Engineering Science

Original Article

Institution of MECHANICAL ENGINEERS
Journal of MECHANICAL ENGINEERING SCIENCE

Proc IMechE Part C:
J Mechanical Engineering Science
2021, Vol. 235(24) 8013–8024

DOI: 10.1177/
09544062211003616
journals.sagepub.com/home/pic
SAGE

Passive shape shifting: A compliant design approach for full film bearings

Joep Nijssen and Ron van Ostayen

Abstract

In tribotronic bearing design active components are used to adapt bearing performance to operating conditions. The principle of self-adaptive bearings has also been presented in literature in which a passive modification of geometry was used for a variation in conditions. This work presents an alternative design approach for self-adaptive bearings. This approach is focused on the shift between two known bearing geometries, where each of them is the preferred solution in a part of the operating regime. Using compliant elements in the bearing design allows for passive shape shifting. Four examples are presented which present this behavior for variable velocity and load conditions. The design approach could possibly provide a cheaper alternative for simple active bearing designs, or could be combined with active components in a tribotronics design to improve existing performance.

Keywords

Shape shifting, tribotronics, full film bearings, compliant mechanisms, self-adaptive, mechanism design

Date received: 19 February 2021; accepted: 24 February 2021

Introduction

Hydrostatic and hydrodynamic slider bearings are classic machine components used for various applications and loading conditions. Traditionally, for analysis purposes they have been assumed to be rigid machine components. Nowadays, the analysis of these types of bearings is significantly more extensive and includes elastic, thermal, rheological, and dynamic effects.[1] Something that simultaneously has been observed is the lack of design innovation in bearing designs.[2] Changing perspectives within engineering, including a more important focus on sustainability and environmentally friendly alternatives provide a stimulus for the tribology community to keep pushing innovation. Efforts are continuously being made in the evaluation of new material combinations, but also continuous innovation within bearing design is necessary. The main approach in this respect still remains to create a monolithic design optimized for one given operation condition.[3–5]

However, hydrostatic and hydrodynamic bearings are used in a wide variety of applications and operating conditions. The Stribeck curve is one visualization method to show the bearing performance for different operating conditions.[6] The general Stribeck curve as seen in Figure 1 can be used to define the operating range of the bearing with respect to friction μ, load W, velocity U, and viscosity η, where the latter three are combined in the characteristic bearing number ζ. Several of the commonly used performance criteria for a bearing can be directly defined by this graph. For example, the term hydrodynamic or hydrostatic lift-off off is used to define the lowest film height at which full film lubrication is obtained.[7–9] This point can be defined by the critical bearing characteristic number ζ_f.

In a typical bearing design problem the operating conditions are described by either a single operating point or by an operating range. In case of an operating range the bearing is designed for a characteristic operation point in that range, perhaps the maximum load or an average load. Here we solely focus on operating ranges with changes in load or velocity, however note that thermal, viscous and counter surface curvature variation are also possibilities. Several load cases and applications can be devised.[10] Harbor cranes can be seen as an example operating condition where the velocity over its operation range might vary, but where the load remains close to constant. An example of operating condition where the velocity remains at a

Department of Precision and Microsystems Engineering, Delft University of Technology, Delft, The Netherlands

Corresponding author:
Joep Nijssen, Department of Precision and Microsystems Engineering, Delft University of Technology, Delft, The Netherlands. Email: j.p.a.nijssen@tudelft.nl

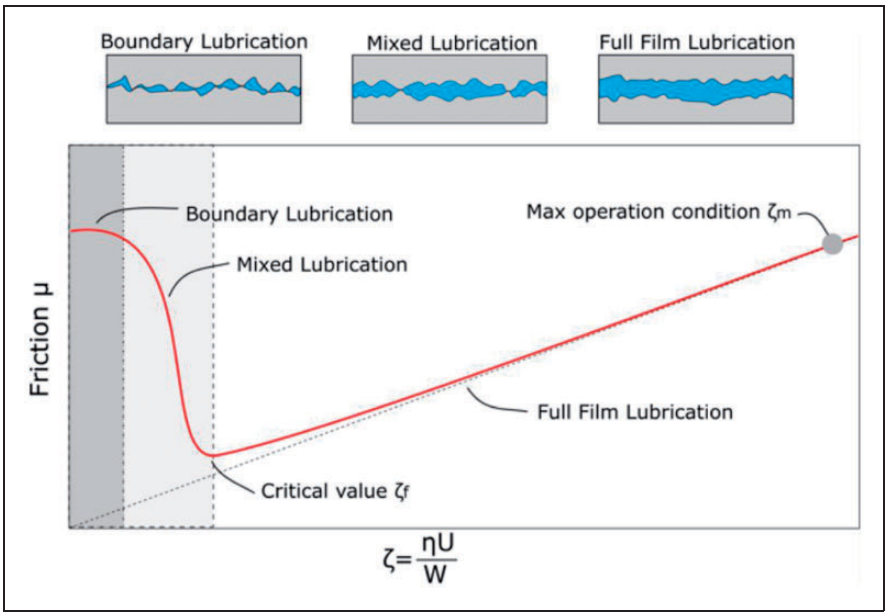

Figure 1. Stribeck curve, defining hydrodynamic bearing performance.

low constant velocity but where the load changes significantly, are for instance moving stadium rooftops with a varying load due to varying winds. Finally, pumps are an example of an application where both the load and velocity can change significantly.[11]

When variable operating conditions are considered in the design of a bearing, more often than not the geometry of the bearing is the limiting factor for the performance, since not every bearing geometry excels in every aspect. This means the bearing designer usually resorts to designing for an average or maximum operating point in the range. There is thus benefit for bearing geometries to be able to change to the current operation condition in the range. A field which is increasingly being investigated is that of tribotronics, the field of so-called active or smart bearings. First defined in Glavatskih and Höglund,[12] the use of mechatronic components enhances the performance range of conventional bearing geometries. An example of performance enhancement using active bearings is improved dynamic stability.[13] They are also used to compensate for changes in operating conditions such as shaft alignment,[14] and orbit regulation.[15] The objective of active bearings in general is to compensate for changes in operating condition through control of factors such as bearing position or pressure sources.[16] Although the possibilities using tribotronics are significant, there are some downsides as well. The addition of actuators, sensors and controllers is a costly investment in general, and the complexity of the system increases. Thus the question arises, how some of this active behavior can be obtained without this increase in system complexity.

Therefor, a different approach is to consider how changes in operating conditions can be handled passively, that is without additional sensors, actuators, or

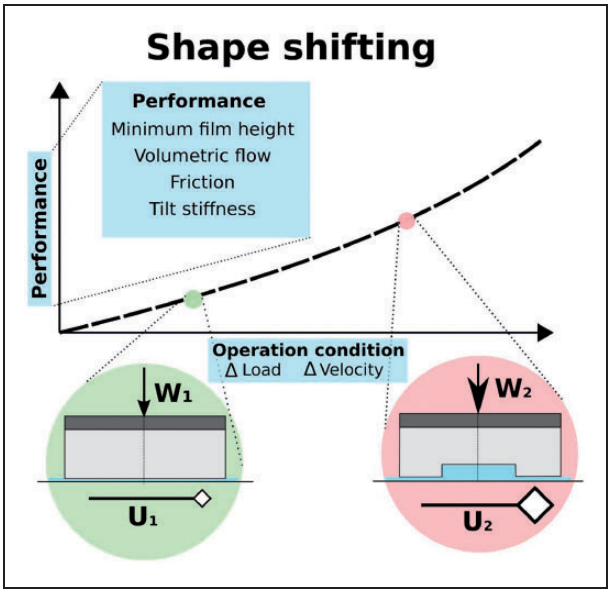

Figure 2. Different operation conditions that can be utilized during passive shape shifting, resulting in changes in possible performance criteria.

control unit. A viable lower cost alternative would be the use of compliant or elastic components. The use of compliance in bearing design can be found in literature in numerous locations, mostly to cope with deformations of the bearing counter surfaces.[17] Other uses have been that of adding a compliant version of a hinge to allow for tilting.[5,18] But examples outside tribology, such as in mechanism design, have shown potential substantial improved performance using compliance.[19] The use of compliance can also be implemented in the design of a passive bearing that can cope with change in operation conditions. This has been seen to some degree in the work by

Jackson et al.,[20–22] where it was referred to as self-adapting surfaces. A second detailed body of work on shape adaptability of bearing using compliance has been performed by Fesanghary et al.[3,23,24] In these types of bearings, the features such as pockets or grooves change in depth in order to adapt to the operation condition. These properties have been utilized both in thrust and journal bearings.

This principle of self-adaptive bearings however can be taken further. By switching between bearing geometries which are known to excel in a certain operation condition, additional performance could potentially be unlocked. In this research we present a method where the bearing is not designed to be optimal in one operating point, but in two selected points in the operating range. This design principle of switching between known bearing shapes, has been defined in this work as the principle of passive shape shifting. This paper presents the potential of this approach to obtain bearings for multi-objective load and velocity operation conditions that can potentially enhance or replace tribotronics. In a set of examples, it will be shown how existing bearing geometries can be combined through the use of elastic elements to capture the essence of the principle.

Method

In this paper we consider the bearing design problem from a multi-objective perspective. This lies at the basis of the passive shape shifting approach, which is to cope with changing operating conditions passively, i.e. without active mechatronic components. It therefore can be used to change the bearing's performance depending on the specific point in the operating condition range as seen in Figure 2. Performance for full film bearings is a broad concept, but usually consist of aspects such as the minimum allowed film height, load capacity, volumetric flow, friction, normal and tilt stiffness. The determination of these performance characteristics requires the evaluation of the pressure profile in the bearing, and thus the solution of the Reynolds equation,[25] which in 1 D form is equal to:

$$\frac{d}{dx}\left(-\frac{h^3}{12\eta}\frac{dP}{dx}+\frac{h}{2}U\right)=0 \tag{1}$$

where h is the film height, P the pressure distribution, η the viscosity and U the velocity of the counter surface. The Reynolds equation inherently captures the coupling between film height, load capacity and volumetric lubricant flow. Depending on the bearing geometry, this results in differences in the aforementioned performance criteria.[26] With passive shape shifting, the bearing uses changes in operating condition, i.e. load and velocity, to change between bearing geometries and thereby obtains a difference in performance. For this approach to be effective, a set of bearing geometries must be identified between which the actual bearing geometry will switch. Literature[26,27] can provide an extensive overview of different geometries and their subsequent performance, of which several have been implemented in this work. The following parameters are used as dimensionless expressions of bearing performance:

$$\bar{h}=\frac{h_{\min}}{L} \tag{2}$$

$$\bar{B}=\frac{q\eta}{P_r h_{\min}^3} \tag{3}$$

$$\bar{\mu}=\frac{1}{UW}\int_0^L\left(\frac{h^3}{12\eta}\left(\frac{dP}{dx}\right)^2+\frac{\eta U^2}{h}\right)\mathrm{d}x \tag{4}$$

which are the dimensionless minimum film height $\bar{h}$ [−], the flow shape factor $\bar{B}$ [−] and friction coefficient $\bar{\mu}$ [−] in accordance with Rowe.[27] They are defined by the minimum film height $h_{\min}$ [m], the bearing length L [m], bearing load $W=\int_0^L P\mathrm{d}x$ [N], viscosity η [Pa·s], output flux q and velocity U [m/s]. The operation conditions are defined by the dimensionless parameters:

$$\bar{W}=\frac{W}{P_s A} \tag{5}$$

$$\bar{\zeta}=\frac{U\eta}{W} \tag{6}$$

where $\bar{W}$ is the dimensionless load, ζ [−] the characteristic bearing number, P_s [Pa] the supply pressure and A [m^2] the bearing area. In case of a hydrostatic bearing that is not subjected to velocity variations, these dimensionless numbers can be used to define the operation condition. The bearing geometry directly influences the performance that is realized depending on the load and velocity operation condition. This becomes more clear when looking at a possible switchable bearing geometry pair as seen in Figure 3. These bearing geometries exhibit distinct differences in pressure profile and therefore load capacity. Given an operation range in which the dimensionless load parameter varies, two performance criteria are utilized, that is the minimum film height $\bar{h}$ [−] and the flow shape factor $\bar{B}$ [−]. Both bearings can be modeled using the 1 D Reynolds equation defined in equation (1). The recess of Figure 3(b). is modeled as having a $L_r = L/10$ in size located symmetrically in the centre of the bearing, with a height $H_r = L/100$. An external pressure source is used with a constant source pressure equal

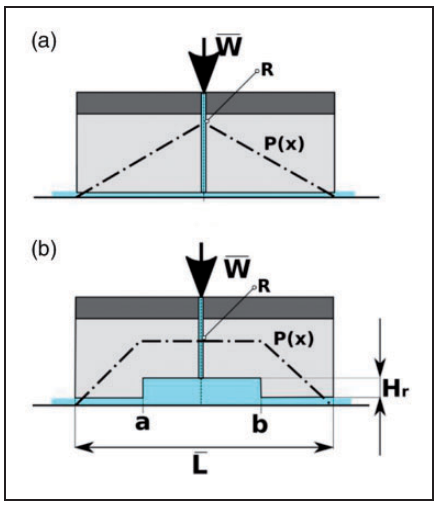

Figure 3. (a) Parallel hydrostatic bearing. (b) Hydrostatic bearing with recess.

to P_s. A linear restrictor (R) is used, which is modeled as:

$$Q_r = \frac{\pi r_r^4}{128\eta}\frac{(P_s - P_r)}{l_r} \tag{7}$$

where $r_r = 0.001L$ and $l_r = 0.02L$. The dimensions of the restrictor are based on having a similar minimum film at the lower bound of the range. The resulting performance for one order of magnitude varying load can be seen in Figure 4. The resulting comparison shows the superiority of the two bearings at different points in the operation range. The parallel bearing, having lower load capacity, has a superior overall flow shape factor and therefore lower volumetric loss. This comes at the cost of having an inferior minimum film height at lower operational loads. This might be crucial in for instance shock loads, causing the bearing to lose its full film capabilities. In that case the recess bearing, with its superior load capacity might be preferred at the cost of a higher temporary flow shape factor.

This fundamentally is the objective of shape shifting, where a varying load case benefits from a change in performance without the use of active components. By moving between the two geometries, the desired performance at both ends of the operational range can be obtained. The following two approaches have been identified as fundamental shape shifting strategies, as visualized in Figure 5. The approaches can be defined as follow:

- Shift of outer geometry: Changing the bearing outer boundary or the dominant bearing boundary.
- shift of feature: Adding or changing the features of bearing surface.

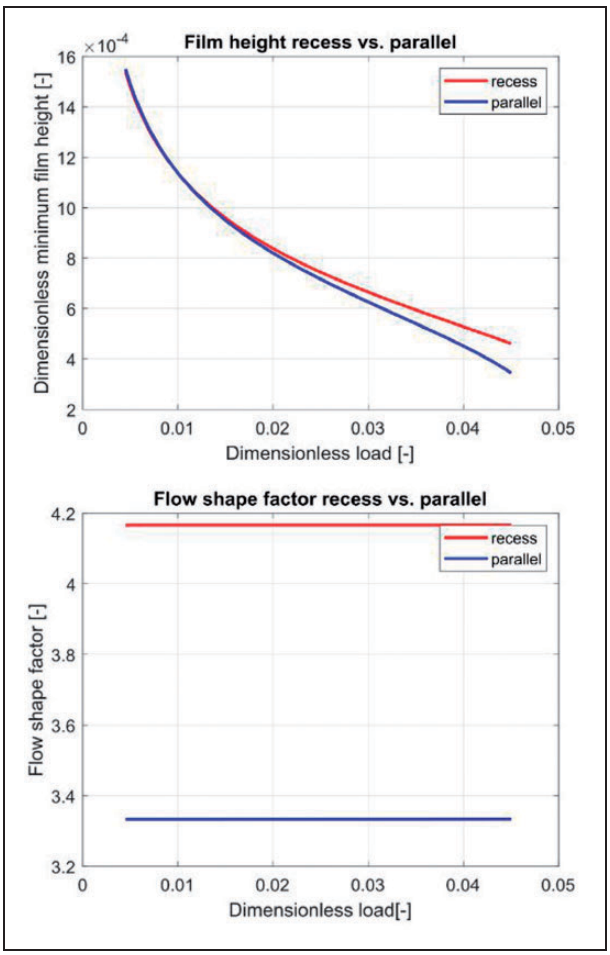

Figure 4. Hydrostatic parallel versus recess bearing in terms of their minimum film height and flow shape factor.

The approaches do not necessarily differentiate in their final objective, but rather possibilities to obtain the same result.

Approach to obtaining passive shape shifting

The primary approach presented in this work to obtain passive shape shifting is through the use of elastic components. The change in operating conditions, i.e. load and velocity, causes changes in the resulting pressure profiles that is acting on the bearing geometry. These changes in location and magnitude of the pressure distribution cause deformation, which in turn can change the bearing geometry and therefore its performance. The implementation of compliant elements to cope with change is analogous to what has been seen in literature,[20,22,24] where linear compliant bearing elements cope with changes in the load condition. Passive shape shifting is a conceptually different design approach in its explicit switch between two different bearing geometries at two locations in the operation range, rather then having features adjust to changes in operation. An example of a compliant shape shifting implementation of Figure 3

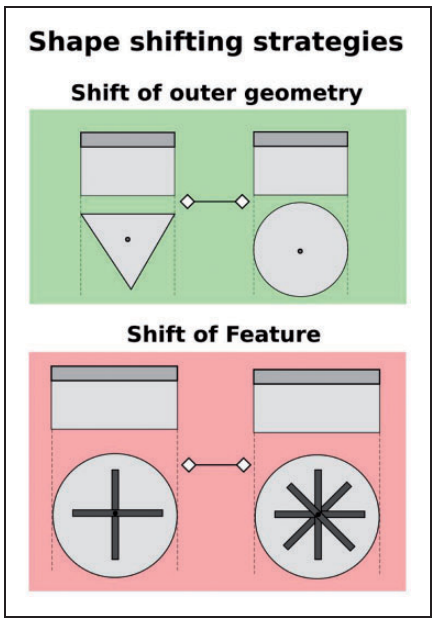

Figure 5. Identified shape shifting strategies. Focus in this work is solely on the shift of feature strategy.

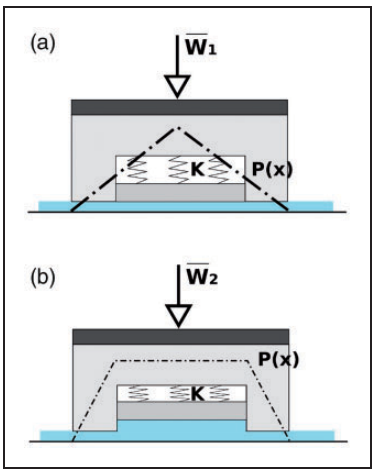

Figure 6. (a) parallel hydrostatic bearing with an elastic element defined by stiffness *K*. (b) Hydrostatic bearing with recess after shape shift. The implementation is presented here in the form of a spring supported separate element in the center of the bearing. A functional embodiment of such an elastic implementation could be similar to the suspended compliant beams that have been observed in,[21,23] a monolithic structure without sliding friction between the pocket and its internal wall.

can be seen in Figure 6. When $\bar{W}_2 > \bar{W}_1$, the increased load can be used to compress the elastic element and therefore passively change the bearing geometry. Implementation of the elastic component thus determines how the shape shifting will occur. Through the use of a number of examples, the potential and design approach will be presented. This work exclusively focuses on using the second design approach, the so-called shift in feature. This design approach takes the preference in this because of its intuitive implementation in existing bearing designs.

Modeling design examples

To show the potential of passive shape shifting, the second design presented in Figure 5 will be used to obtain different shape shifting bearing designs. The examples will either be load or velocity dependent, meaning the operation range will either be represented by the dimensionless load $\bar{W}$ for hydrostatic bearings or the characteristic bearing number $\bar{\zeta}$ for hydrodynamic bearings. The examples will share the following common traits:

1. The main dimension will be expressed by a characteristic bearing length $\bar{L} = 1$ [−].
2. Any elastic elements used within the bearing surface are modeled as both geometrically linear as well as possessing a linear elastic material model.
3. The examples will be presented in their lowest possible geometrical embodiment. This means they will modeled in 1D if possible.

The modeling of the primary bearing examples using the finite element method has been studied and described in literature extensively over the past 40 years.[28] In addition, the focus in this work is the design approach, and thus a finite element approach generally suffices for first concept validity. The examples are all modeled using Comsol Multiphysics V5.5. Here the Reynolds equation is defined using the general form partial differential equation toolbox. In the examples the geometrical embodiment is used with the smallest dimension. And thus the majority of examples are defined purely as a line, with the space between nodes defining pockets. This is done as such since solely the domain between the fluid and bearing is modeled. All examples are modeled as quasi static, meaning time dependent effects such as squeeze are not taken into account. This means the Reynolds equation on the majority of examples is defined as described in equation (1). In case of a 2 D geometry, the Reynolds equation is defined as follows:

$$\frac{\partial}{\partial x}\left(-\frac{h^3}{12\eta}\frac{\partial P}{\partial x}+\frac{h}{2}U\right)+\frac{\partial}{\partial y}\left(-\frac{h^3}{12\eta}\frac{\partial P}{\partial y}+\frac{h}{2}V\right)=0 \tag{8}$$

Where U and V are the velocities in x and y direction, respectively. The film height can be described using a function that includes all possible potential groove shapes and that will be specified for each example that follows. For all examples the solution for the film height will be found by solving to find load equilibrium:

$$W=\int_A P\mathrm{d}A \tag{9}$$

Where A is either a surface (x, y) or a region (x) depending on the dimension of the geometrical embodiment. This means both the general form PDE and global ODE physics of Comsol have been implemented. Note that the models are not necessarily optimized. Instead the objective of this work is to provide a viewpoint on the potential of passive shape-shifting as a design approach. Four examples are presented in the next section, each with a specific set of operating point combinations and therefore bearing design concepts to be merged in one shape shifting design.

Example 1: Tilting rayleigh step

This example is based on the change of dominant bearing geometry and consists of the combination of the well known Rayleigh step bearing and tilting pad bearing seen in Figure 7. The Rayleigh step is known as the bearing geometry with the highest hydrodynamic load capacity of all bearing geometries.[29] It is thus highly suited as a geometry to be used for good hydrodynamic lift-off properties, in order to minimize the ζ_f value in Figure 1. The Rayleigh step is a fixed sized bearing geometry as seen in Figure 7. The tilting pad, on the other hand is a geometry that is dependent on the relative film height and therefore changes depending on the load condition. Both bearing geometries are analyzed using the 1 D Reynolds equation. In the case of the Rayleigh step the film height h_r is defined as:

$$h_r = h_0 + f(x) \tag{10}$$

where $f(x)$ is a step function with location of the step at L_s and with a step height of r_s. The optimal values for such a geometry are known.[30] m The film height of the tilting pad h_t can be defined as follows:

$$h_t = h_0\Big(1 + a(1-x)\Big) \tag{11}$$

with a the dimensionless angle parameter. This parameter can be solved by determining the equilibrium of load and of moment and by setting the eccentricity value e equal to the optimal value of $0.077L$.[30] This moment equilibrium needs to be solved simultaneously with the load equilibrium and can be defined as:

$$W\left(\frac{L}{2} + \epsilon\right) = L^2 \int_x (Px)\mathrm{d}x \tag{12}$$

Because the Rayleigh step has a fixed geometry, it does not conform to the new load condition as a result of the increased counter surface velocity. At higher velocity, where the minimum film height is usually of less importance compared to the friction, its performance falls behind compared to the tilting pad. By combining the Rayleigh step and the tilting pad in one bearing using the passive shape shifting approach, both the superior friction aspect of the tilting pad at high velocity as well as the higher minimum film height of the Rayleigh step at low velocity can be realized. The resulting combination can be seen in Figure 8. This combination has already been investigated before in literature[31] in order to reduce friction over the operating range, but it is also an excellent example that shows the promise of passive shape shifting behavior. The principle behind this bearing is that it behaves like a Rayleigh step at low characteristic bearing values, while acting like a tilting pad at higher characteristic values. Note that this

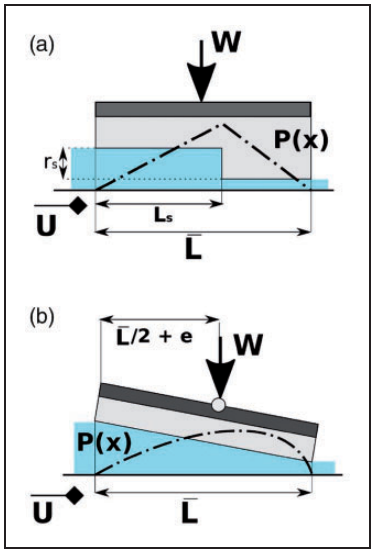

Figure 7. (a) Rayleigh step with all design parameters denoted. (b) a conventional tilting pad. with all design parameters denoted.

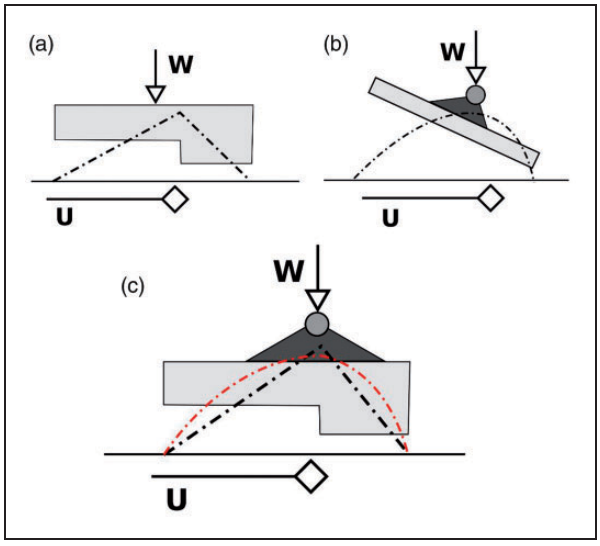

Figure 8. (a) Rayleigh step and (b) conventional tilting pad. They have been combined in (c) as the tilting Rayleigh step concept.

tilting of the Rayleigh step may result in wear of the feature and eventual loss of potential improved performance. The hinge in the tilting center, which conventionally has been realized in a knife-edge configuration, can also be made using a compliant element. This has been found in literature in different designs, such as flexure based[20,31] and through elastic rubber material.[5] The main advantage of the second embodiment is its use in water-hydraulic systems.[5]

Example 2: Parallel to recess bearing

In the second example the previously presented parallel and recess bearing geometries are combined with the implementation of an elastic component as seen in Figure 6. The hydrostatic bearing with an elastic recess pocket is subjected to a variable load. The bearing is again modeled using the 1 D Reynolds equation. The film height in this case is defined by the following function:

$$h_h = A_r(H(x-a) - H(x-b)) + h_0 \tag{13}$$

where $H(x)$ is the Heaviside function, a and b are the outer locations of the virtual recess and A_r is the depth of the recess and h_0 is the minimum film height. This function is used to imitate the bearing profile of Figure 3(b). The boxcar function $\Pi_{bc} = H(x-a) - H(x-b)$ defines the virtual pocket, where the amplitude of the recess is directly coupled to the stiffness of the virtual spring K_r. In this example, the stiffness is coupled to the normalized load case as $K_r = (2\text{E}5 \cdot \bar{W}_1/\bar{L})$ with $\bar{W}_1$ being the initial dimensionless load of the operation range. The remaining part of the bearing surface is considered infinitely stiff. By iteration both for the balance of global load $W - W_0$ as well as local recess load W_r, the performance of the bearing can be identified. The location of the virtual pocket is $a = -0.05L$ and $b = 0.05L$ respectively. This means the load on the recess surface can de described as:

$$W_r = \int_a^b P(x)dx \tag{14}$$

And the resulting virtual pocket load equilibrium as:

$$W_r = K_r A_r \tag{15}$$

Example 3: Parallel to tilt recess bearing

Similar to the previous example, pockets are added into the bearing surface. The newly obtained performance however is the increase of tilt stiffness at higher loads, by placing two additional pockets as seen in Figure 9. The film height of this 1 D bearing concept can de modeled as:

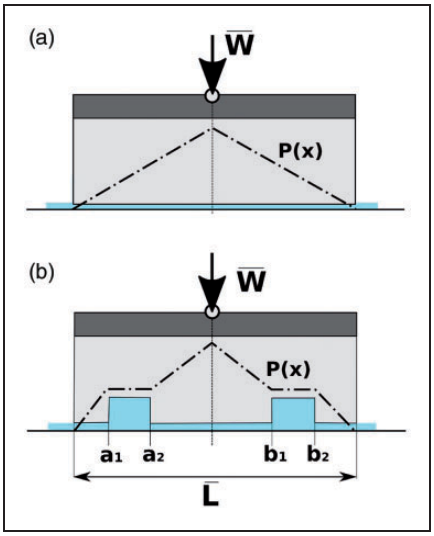

Figure 9. Pressure profile of the parallel bearing and subsequent pocket bearing that increases tilt stiffness.

$$h_h = h_{rl} + h_0 + h_{rr} \tag{16}$$

With h_{rl} and h_{rr} are the film height functions of the left and right pocket respectively, defined as:

$$h_{rl} = A_{rl}(H(x-a_1) - H(x-a_2)) \tag{17}$$

$$h_{rr} = A_{rr}(H(x-b_1) - H(x-b_2)) \tag{18}$$

For the example presented, $a_1 = -0.4L$, $a_2 = -0.3L$, $b_1 = 0.3L$ and $b_2 = 0.4L$. The same approach to determine the equilibrium between the local load and the spring stiffness is described by equations (14) and (15) respectively. To determine the effect the pockets have on the tilt stiffness of the bearing at higher operational load, an external moment can be applied. This external moment can be defined as:

$$\bar{M}_{ex} = \bar{W}\epsilon \tag{19}$$

Where ϵ is the relative eccentricity [–] of the load relative to the bearing center.

Example 4: 4 to 8 lubricant groove bearing

Radial lubricant grooves have been implemented in literature as ways to feed the entire bearing surface with lubricant, in combination with an increase in load capacity. Because of the nature of the features, a 2 D geometry is needed to study this concept, and the bearing is thus modeled using the 2 D Reynolds equation defined in equation (8). In this example the shape shifting bearing will switch between its 4 and 8 lubricant grooves embodiments. The bearing geometries as

well as their pressure profiles for these two embodiments can be seen in Figure 10.

The dimensions of the rectangular lubricant grooves are $L_o = 5/16\bar{L}$ and $W_{groove} = 1/30\bar{L}$. The

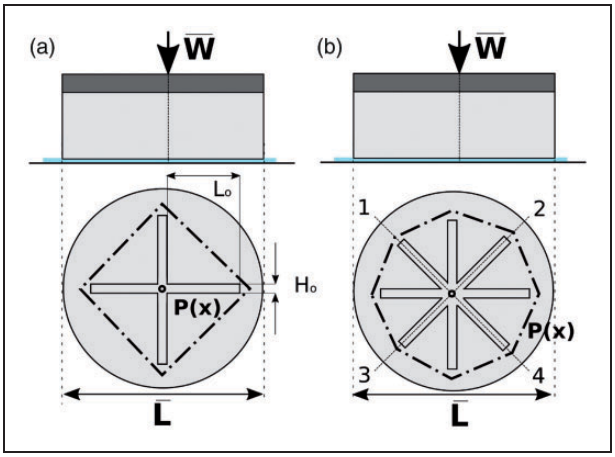

Figure 10. 2 D lubricant groove bearing with its 4-groove and 8-groove configuration. The lubricant grooves that have elastic characteristics are denoted by numbers 1 to 4.

are oriented symmetrically with respect to the bearing center, with angles of 90 degrees and 45 degrees for the 4 and 8 groove embodiment respectively. The depth of the rigid grooves are given by $H_o = \bar{L}/100 + h_0$. The depth of the elastic grooves is defined by the equilibrium of the spring force W_r and the integral of the pressure over the groove surface, similar to the steps performed in the previous examples. Finally, stiffness of the elastic grooves equals $K_r = 1\text{E}5\bar{W}_1/\bar{L}$.

Results

All 4 presented examples have been analyzed using the finite element analysis software Comsol Multiphysics. In all cases an operation range is chosen of at least one order of magnitude difference between the lowest and highest operation value. The pressure profiles for these two operation points in the range are presented in Figure 11. In all cases the rigid counterparts of shape shifting bearings are also presented to show the improvement in performance.

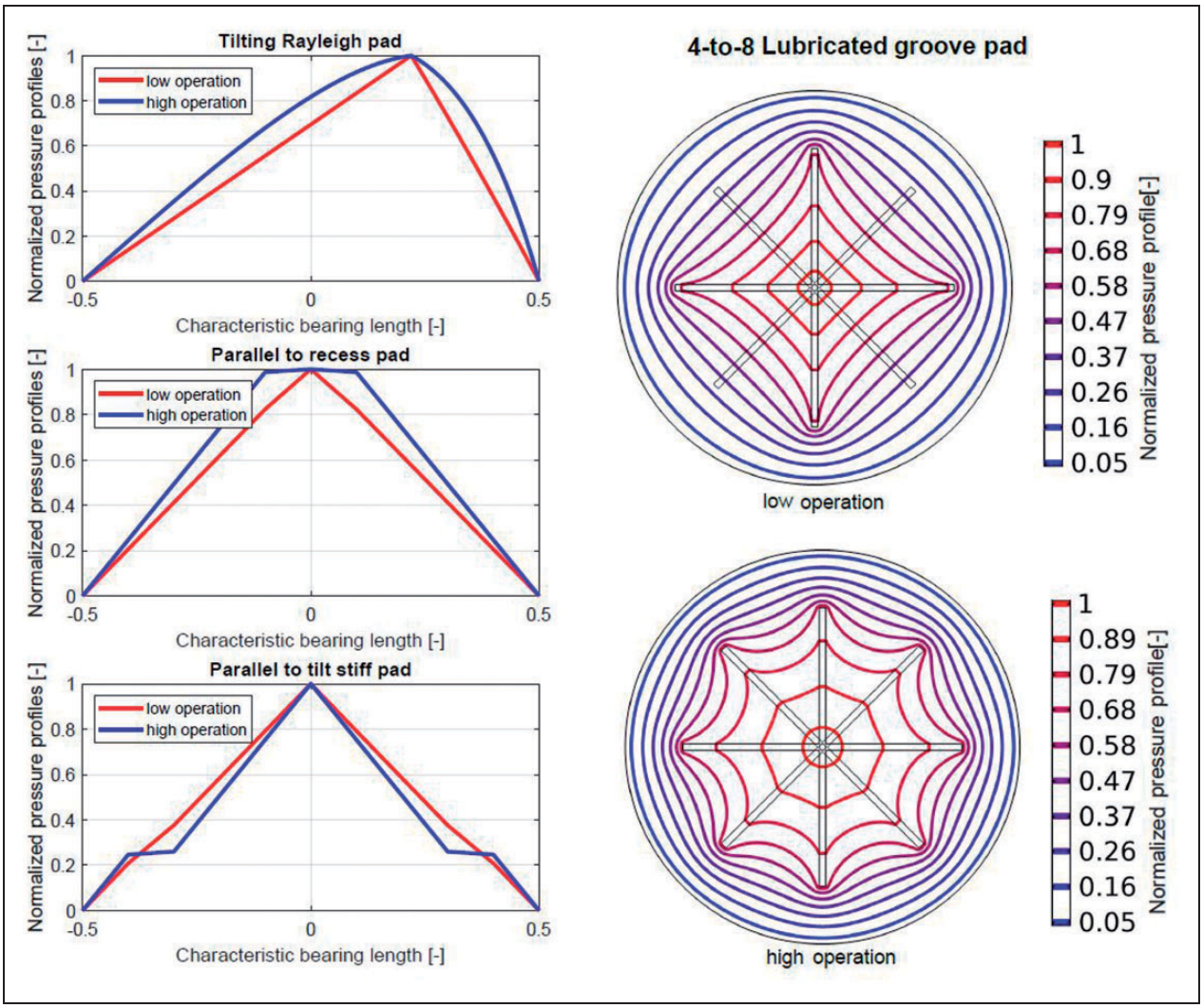

Figure 11. The normalized pressure profiles of all 4 concepts at both ends of their operation regime.

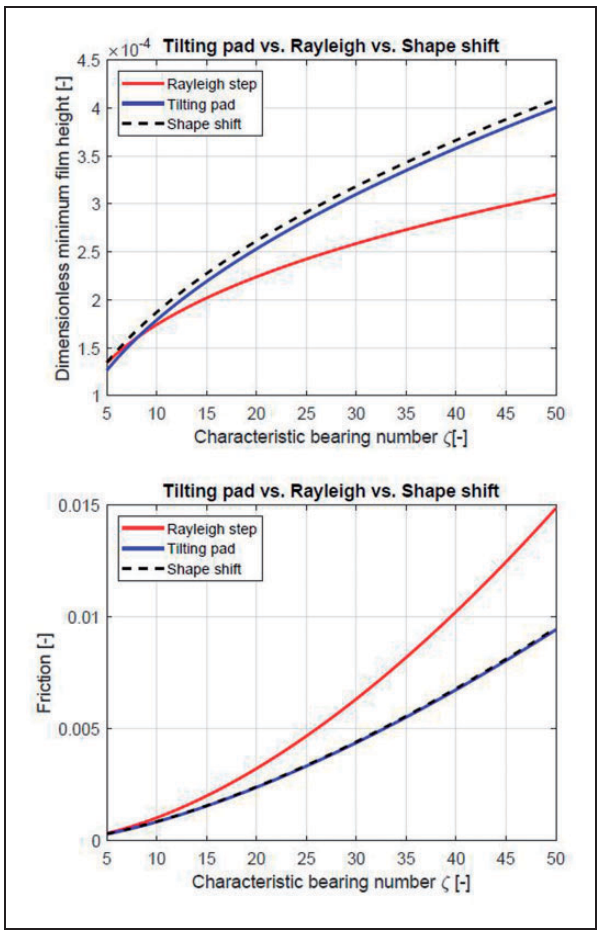

Figure 12. The Rayleigh step vs. tilting pad vs. its shape shifting variant. Both the minimum film height of the bearings as well as the friction coefficient are given for an operation range varying one order of magnitude.

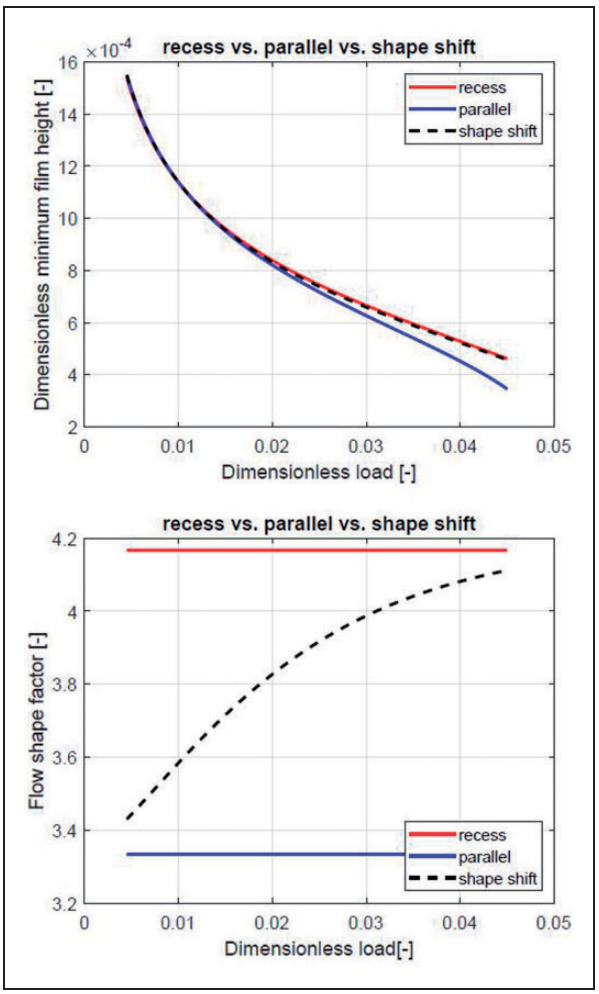

Figure 13. The parallel vs. recess pad vs. its shape shifting variant. Both the minimum film height of the bearings as well as the flow shape factors are given for an operation range varying one order of magnitude.

Tilting rayleigh pad

The resulting behavior can be seen in Figure 12. The shape shifting bearing at $\zeta = 5$ has a 0.61% increase in minimum film height with respect to the conventional Rayleigh step, but a 12.77% increase of film height with respect to the tilting pad. At higher operation, the shape shifting bearing follows the performance of the tilting pad with only a 0.77% higher friction coefficient then its tilting pad counterpart. The angle parameter $a = 1.179$ for the conventional tilting pad. The shape shifting variant however has a constantly varying tilt angle, with the minimum tilt parameter being $a = 0.062$ at the lower bound of the range and $a = 0.829$ at the higher bound of the range.

Parallel to recess pad

In this concept the objective of the shape shifting version was to operate as a parallel bearing at low operational load, and thus low flow, and with a higher load capacity at higher operational load. Comparison between the bearings can be seen in Figure 13. The bearing has at low operational load $\bar{W}_1 = 0.0045$ a 2.91% increase in flow shape factor with respect to the parallel pad. At high operational load, the shape shifting bearing has a 1.07% lower film height then its recess counterpart.

Parallel to tilt stiff pad

The resulting comparison can be seen in Figure 14. At low operational load the difference in flow shape factor between the shape shifting bearing and its parallel counterpart is equal to 4.08%. At higher loads the increased tilt stiffness is desired. The dimensionless rotation stiffness K_r is defined by the slope, which equals 7.46, 7.18 and 5.46 for the recess, shape shift and parallel bearings respectively. There is thus only a 3.75% decrease in stiffness between the rigid recess and shape shifting bearings.

4 To 8 lubricant groove pad

The results of the groove bearing analysis can be seen in Figure 15. At low operational load $\bar{W}_1 = 0.05$ the difference in flow shape factor between the 4-groove and shape shifting bearing is 1.1%. At the high

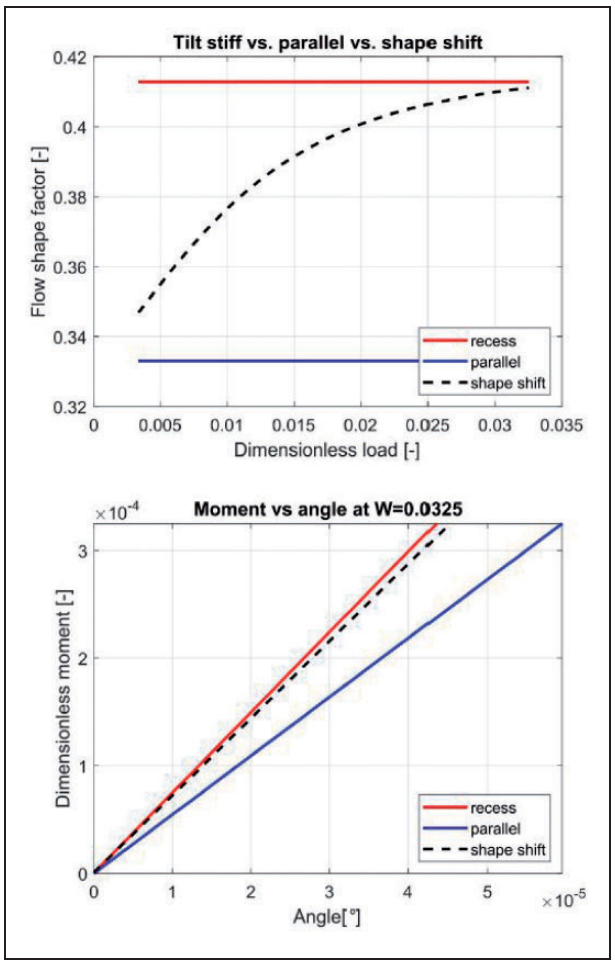

Figure 14. The parallel vs. tilt stiff pad vs. its shape shifting variant. Both the flow shape factors of the bearings as well as the moment-rotation curves are given for an operation range varying one order of magnitude.

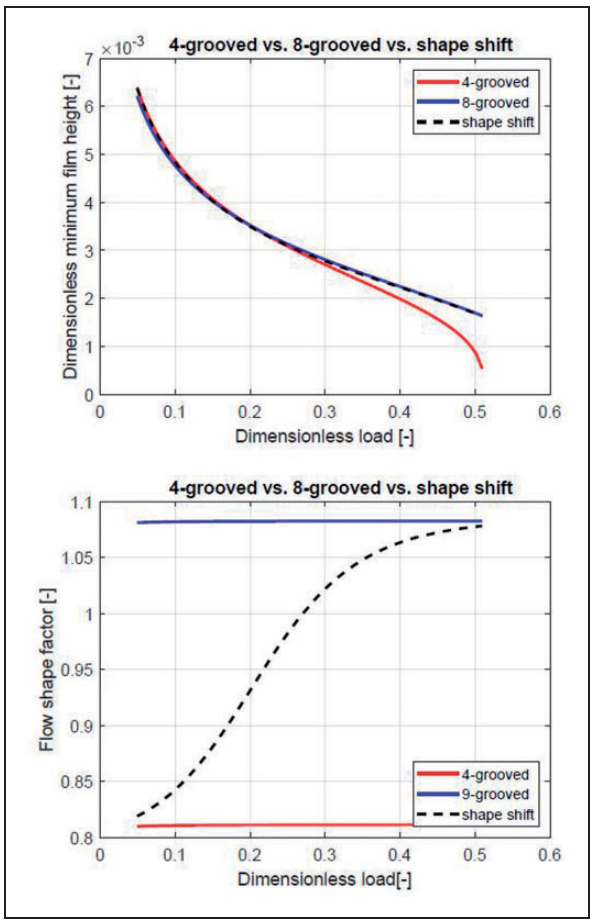

Figure 15. The 4-groove vs. 8-groove vs. its shape shifting variant. Both the minimum film height of the bearings as well as the flow shape factors are given for an operation range varying one order of magnitude.

operation, the difference between the rigid 8-lubricated groove and shape shifting variant is 0.49% respectively.

Discussion

Four examples were presented in this work to show the possibilities of passive shape shifting. The tilting Rayleigh pad bearing is the only example where the shift in shape is the result of changing pressure profile as a result of a variation in velocity. We can observe from the results that the introduction of the shape shifting variant forces us to accept some minor compromises. This is seen in the slightly higher friction for the higher end of the operating range. Note also the difference in bearing angle, in that the shape shifting variant is less tilted compared to the conventional tilting pad. As result of a velocity variation, the magnitude of the pressure does not change significantly, however the location of the pressure peak does change. It is expected that this change is less significant then a shift in pressure profile that is the result of a load change.

The other three examples exhibit shape shifting as result of a load changing operation condition. In all cases the switching results in a clear visible change in flow shape factor. Because these examples are force controlled, it is expected that the shifting properties in these bearing types are more dominant. The load variation operating condition is inherently an easier condition to utilize when working with elastic elements, because of the fundamental coupling between load and displacement through element stiffness.

This means that the design for passive shape shifting with velocity variation is inherently less intuitive, and the passive effects are less significant in terms of shifting capabilities. The examples presented in this paper are also limited by the use of linear stiffness elements. The effective operation range could potentially be increased or decreased further through the addition of non-linear or pre-loaded stiffness elements. Non-linear stiffness elements are already widely investigated to increase the performance of other compliant mechanisms.[19] The relatively small scale of the required elements and their displacement range prove be a challenge, although micro

mechanisms with comparable characteristics can also be found in Literature.[32]

Finally a reflection on some of the modeling simplifications and their impact on the solutions provided is made. The introduced examples are all modeled by introducing the effects of elasticity into the Reynolds equation and by neglecting thermal effects, variations in viscosity and structural dynamics. In particular thermal effects could influence the deformation effects that are at the basis of the presented method. The reasons thermal effects have not been taken into account in the presented examples are two-fold. First, the choice for this was made based on the desire to introduce the design method and therefore solely apply simple models and the minimum required physics to show the design potential. Second, the effects thermal deformation on full film bearings is heavily dependent on the design case, dimensions and bearing topology. Thermal deformation has been seen in literature to cause significant deformation, although this is especially critical for larger hydrodynamic journal bearings where the film height is small,[33,34] and where the deformation magnitude is also seen to be around or less than the magnitude of the intended minimum film height.[33,35] This means that these effects might effect the lower operation conditions where parallel bearing surfaces are desired, but are less critical in the high operation condition where the elastic deformation amounts to several times the minimum film height.

Conclusion

This work has presented a different design approach to design for variable operation conditions, introduced as passive shape shifting. Analogous to self-adaptive bearings, compliant elements are used to obtain movement in the bearing surface. Different to self-adaptive bearings as described in literature, here two dominant bearing geometries are chosen beforehand, making it possible to switch between them both and utilizing both dominant geometries over an operating range. This can be used to design for different objectives within the operation range, such as low ζ_f hydrodynamic lift-off, lower friction, increased tilt stiffness, or decreased volumetric flow. The preliminary insight for the method is that design for variable load conditions is more intuitive when using compliant elements compared to variable velocity conditions. Primary future objectives are the further development and validation of these type of bearings using experiments and their comparison with active bearing designs.

Future work

Since this work focuses on the conceptual embodiment of the shape shifting principle, future steps are required to better validate the potential of the approach. One of the main future objectives is validation through experimental validation. This implementation would be most beneficial into systems that have two clear distinctive operation cases within their operation cases, such as hydraulic pumps[11,36] that have a clear distinction between their compression and filling strokes. A secondary important point of future emphasis should be the specific embodiments used for the compliant elements within the bearing surface, that in this work have been solely treated as a linear spring. Although several embodiments can be found in literature of potential elastic grooves and pockets,[21,23] the requirement for relatively large motions compared to the film height might require the investigation of alternatives. Investigating the solutions provided in the field of compliant mechanisms[19] might provide us with simple and elaborate options.

Declaration of Conflicting Interests

The author(s) declared no potential conflicts of interest with respect to the research, authorship, and/or publication of this article.

Funding

The author(s) received no financial support for the research, authorship, and/or publication of this article.

References

1. Liu Z, Wang Y, Cai L, et al. A review of hydrostatic bearing system: researches and applications. *Adv Mech Eng* 2017; 9: 168781401773053–27.
2. Lampaert SG, Quinci F and van Ostayen RA. Rheological texture in a journal bearing with magneto-rheological fluids. *J Magnet Magnet Mater* 2020; 499: 166218.
3. Fesanghary M and Khonsari MM. On the optimum groove shapes for load-carrying capacity enhancement in parallel flat surface bearings: theory and experiment. *Tribol Int* 2013; 67: 254–262.
4. Rohde SM. The optimum slider bearing in terms of friction. *J Tribol* 1972; 94: 275–279.
5. Liang X, Yan X, Ouyang W, et al. Thermo-elasto-hydrodynamic analysis and optimization of rubber-supported water-lubricated thrust bearings with polymer coated pads. *Tribol Int* 2019; 138: 365–379.
6. de Kraker A, van Ostayen RA and Rixen DJ. Calculation of stribeck curves for (water) lubricated journal bearings. *Tribol Int* 2007; 40: 459–469.
7. Lu X and Khonsari MM. On the lift-off speed in journal bearings. *Tribol Lett* 2005; 20: 299–305.
8. Heinrichson N and Santos IF. Reducing friction in tilting-pad bearings by the use of enclosed recesses. *J Tribol* 2008; 130: 1–9.
9. van Ostayen RAJ, van Beek A and de Kraker A. Lift-off of the hydrostatic thrust bearing with elastic surfaces. In: *2004 AIMETA International Tribology COnference*, Rome, Italy, 14–17 September, 2004, pp. 491–498. Aracne.
10. Neale M. *Tribology handbook*. 1 ed. Oxford: The Butterworth group, 1973.

11. Mulders SP, Frederik N and Diepeveen B. Control design, implementation, and evaluation for an in-field 500 kW wind turbine with a fixed-displacement hydraulic drivetrain. *Wind Energ Sci* 2018; 3: 615–638.
12. Glavatskih S and Höglund E. Tribotronics-towards active tribology. *Tribol Int* 2008; 41: 934–939.
13. Tůma J, Šimek J, Škuta, et al. Active vibration control of hydrodynamic journal bearings. J *Springer Proc Physics* 2011; 139: 425–431.
14. Rehman WU, Jiang G, Luo Y, et al. Control of active lubrication for hydrostatic journal bearing by monitoring bearing clearance. *Adv Mech Eng* 2018; 10: 168781401876814–17.
15. Deckler D, Veillette R, Braun M, et al. Simulation and control of an active tilting-pad journal bearing. *Tribol Trans* 2004; 47: 440–458.
16. Varela AC and Santos IF. Tilting-pad journal bearings with active lubrication applied as calibrated shakers: theory and experiment. *J Vibr Acoust Trans ASME* 2014; 136: 1–11.
17. Van Ostayen RA, Van Beek A and Ros M. A parametric study of the hydro-support. *Tribol Int* 2004; 37: 617–625.
18. Van Beek A and Segal A. Rubber supported hydrostatic thrust bearings with rigid bearing surfaces. *Tribol Int* 1997; 30: 47–52.
19. Howell L. *Compliant mechanisms*. Hoboken, NJ: Wiley & Sons, 2001.
20. Jackson R and Lei J. Hydrodynamically lubricated and grooved biomimetic self-Adapting surfaces. *J Funct Biomater* 2014; 5: 78–98.
21. Duvvuru RS, Jackson RL and Hong JW. Self-adapting microscale surface grooves for hydrodynamic lubrication. *Tribol Trans* 2008; 52: 1–11.
22. Jackson RL. Self adapting mechanical step bearings for variations in load. *Tribol Lett* 2005; 20: 11–20.
23. Fesanghary M and Khonsari MM. On the shape optimization of self-adaptive grooves. *Tribol Trans* 2011; 54: 256–264.
24. Fesanghary M and Khonsari MM. On the modeling and shape optimization of hydrodynamic flexible-pad thrust bearings. *Proc IMechE, Part J: J Engineering Tribology* 2013; 227: 548–558.
25. Downson D. A generalized Reynolds equation for fluid-film lubrication. *Int J Mech Sci* 1962; 4: 159–170.
26. Balcerzak MJ and Raynor S. Solutions for several shapes of externally pressurized hydrostatic thrust bearing. *Appl Sci Res* 1962; 11: 189–217.
27. Rowe WB. *Hydrostatic, aerostatic and hybrid bearing design*. 1st ed. Amsterdam: Elsevier, 2013.
28. Aurelian F and Bonneau D. Finite element method for fluid film bearings. In: Jane Wang Q and Chung YW (eds) *Encyclopedia of tribology*. Berlin: Springer, 2013, pp.34–109.
29. Hamrock BJ and Anderson WJ. Rayleigh step journal bearing, part II-Incompressible fluid. *J Lubr Technol* 1969; 91: 641–650.
30. van Beek A. *Advanced engineering design lifetime performance and reliability*. 6th ed. Netherlands: TU Delft, 2015.
31. Heinrichson N. *On the Design of Tilting-Pad Thrust Bearings*. PhD dissertation, Technical University of Denmark, 2007.
32. Kuppens PR, Herder JL and Tolou N. Permanent stiffness reduction by thermal oxidation of silicon. *J Microelectromech Syst* 2019; 28: 900–909.
33. Lu D, Liu K, Zhao W, et al. Thermal characteristics of water-lubricated ceramic hydrostatic hydrodynamic hybrid bearings. *Tribol Lett* 2016; 63: 1–10.
34. Laukiavich CA, Braun MJ and Chandy AJ. An investigation into the thermal effects on a hydrodynamic bearing's clearance. *Tribol Trans* 2015; 58: 980–1001.
35. Chalkiopoulos M, Charitopoulos A, Fillon M, et al. Effects of thermal and mechanical deformations on textured thrust bearings optimally designed by a THD calculation method. *Tribol Int* 2020; 148: 106303.
36. Harris RM, Edge KA and Tilley DG. Predicting tlie beliavior of slipper pads in swashplate-type axial piston pumps. *J Dyn Syst Measure Control Trans ASME* 1996; 118: 41–47.